

NMR observations of molecular motions and Zeeman-quadrupole cross relaxation in 1,2-difluorotetrachloroethane^{a)}

Harold T. Stokes,^{b)} Thomas A. Case, and David C. Ailion

Department of Physics, University of Utah, Salt Lake City, Utah 84112

C. H. Wang

Department of Chemistry, University of Utah, Salt Lake City, Utah 84112

(Received 6 November 1978)

We report measurements of ^{19}F NMR relaxation times T_1 , $T_{1\rho}$, T_{1D} , and T_2 in the plastic crystal $\text{CFCl}_2\text{-CFCl}_2$. From the data near the melting point, we obtain the jump time for translational self-diffusion. At lower temperatures, we observe on the cold side of the T_1 and $T_{1\rho}$ minima an unusual field dependence which is substantially less than the normal field-squared dependence. We also observe a reduction in T_1 near 40 MHz due to cross relaxation between the Zeeman levels of the ^{19}F spins and quadrupole levels of the ^{35}Cl and ^{37}Cl spins. We measured the cross relaxation times τ_{IS} as a function of field and found good agreement with our theoretical calculation of τ_{IS} .

I. INTRODUCTION

Solids composed of molecules of approximate spherical shape often form a plastic crystalline phase (as defined by Timmermans¹) prior to melting. In such a phase, the molecules sit in a regular lattice, usually cubic, but reorient rapidly in a manner characteristic of a liquid. Thus, a plastic crystal exhibits translational order but orientational disorder.

At some lower temperature T_t , the crystal undergoes an order-disorder transition below which the orientation of the molecules becomes ordered. It is possible normally to supercool the plastic crystal below T_t by lowering the temperature rapidly. In a few cases² where this has been done, a glass phase transition has been observed at a temperature $T_g < T_t$, below which a glassy crystalline phase (as defined by Adachi *et al.*³) is formed. Such glassy crystals are in a metastable state in which the rate of molecular reorientation becomes so small that a transition to the more thermodynamically stable ordered crystalline state is not observed over the time scale of a given experiment.² Thus the molecules are "frozen" into a state of orientational disorder.

The compound $\text{CFCl}_2\text{-CFCl}_2$ forms a plastic crystalline phase below its melting point $T_m = 298^\circ\text{K}$. The order-disorder phase transition occurs at $T_t = 170^\circ\text{K}$. However, the plastic crystalline phase is so easily supercooled that the ordered crystalline phase is difficult to achieve.^{4,5} In the supercooled plastic crystalline phase, a glass phase transition occurs at $T_g = 90^\circ\text{K}$ below which molecular reorientations are frozen out.^{4,5} Another relaxation phenomenon was observed in heat capacity measurements^{4,5} at 130°K and has been

ascribed to the freezing of conversion between the *trans* and *gauche* conformers of the molecule.

In this paper, we report NMR measurements in $\text{CFCl}_2\text{-CFCl}_2$ from its melting point T_m down to 77°K . We interpret our results in terms of molecular motions (e.g., translational self-diffusion near T_m and molecular reorientations at lower temperatures). In addition, we observe cross relaxation between the Zeeman energy levels of ^{19}F and the quadrupole levels of ^{35}Cl and ^{37}Cl . We compare our data with a theoretical calculation of the cross relaxation time and find good agreement.

Previous NMR measurements in $\text{CFCl}_2\text{-CFCl}_2$ have been made by others: namely second moments^{6,7} and linewidth measurements⁴ as well as T_1 and $T_{1\rho}$ relaxation times.⁴ We compare our results with these wherever applicable.

II. SECOND MOMENT CALCULATION

The structure of the $\text{CFCl}_2\text{-CFCl}_2$ molecules has been determined by electron diffraction⁸ from which the position coordinates of the atoms are obtained (see Table I). In the solid phase, these molecules lie in a body-cen-

TABLE I. The position coordinates of the atoms in a $\text{CFCl}_2\text{-CFCl}_2$ molecule for the two isomers. The z axis is chosen along the C-C bond with the origin at the midpoint.

Atom	Position (in Å)					
	<i>trans</i>			<i>gauche</i>		
	x	y	z	x	y	z
C	0	0	0.77	0	0	0.77
C	0	0	-0.77	0	0	-0.77
F	1.31	0	1.18	1.31	0	1.18
F	-1.31	0	-1.18	0.67	1.12	-1.18
Cl	-0.76	1.45	1.43	-0.76	1.45	1.43
Cl	-0.76	-1.45	1.43	-0.76	-1.45	1.43
Cl	0.76	1.45	1.43	0.85	-1.39	-1.43
Cl	0.76	-1.45	-1.43	-1.63	0.10	-1.43

^{a)}A preliminary report of the results contained in this paper was presented in September 1978 at the XXth Ampère Congress in Tallinn, USSR and will appear in the proceedings of that conference.

^{b)}Current address: Department of Physics, University of Illinois, Urbana, Illinois 61801.

TABLE II. Contributions to the second moment (in G²) of the ¹⁹F NMR line shape.

		Intramolecular		Intermolecular		Chemical shift anisotropy	Total
		F-F	F-Cl	F-F	F-Cl		
Isotropic Rotation		0	0	0.134	0.006	0	0.140
Rigid	<i>Trans</i>	0.16	0.073	0.32	0.016	0.18	0.75
Lattice	<i>Gauche</i>	0.84	0.063	0.32	0.016	0.18	1.44

tered cubic (bcc) lattice with a cell constant $a_0 = 7.18 \pm 0.04$ Å at 15°C as determined by x-ray diffraction.^{4,5} (The cell constant a_0 is defined to be the distance between lattice points along the [100] direction.)

In calculating the second moment of the NMR line shape, we consider two cases. The first case is the plastic crystalline phase. In this phase, the molecules reorient very rapidly; hence, the nuclear dipolar spin-spin interaction is averaged over the motion. If we assume the reorientations to be isotropic, we find that the intramolecular interactions average to zero. The intermolecular interactions, on the other hand, average to a value which can be calculated exactly by placing all nuclear spins at the centers of their respective molecules.⁹⁻¹¹ Thus we readily obtain expressions for the second moment of the ¹⁹F line shape due to I - I interactions (I refers to ¹⁹F spins),

$$M_{2II} = 2 \times 3I(I+1)\gamma_I^2 \hbar^2 a_0^{-6} S_1, \quad (1)$$

and that due to I - S interactions (S refers to ³⁵Cl or ³⁷Cl spins),

$$M_{2IS} = 4f_s \frac{4}{3} S(S+1)\gamma_S^2 \hbar^2 a_0^{-6} S_1. \quad (2)$$

In the above expressions, γ_I and γ_S are the gyromagnetic ratios of the I and S spins, respectively; f_s is the fractional abundance of the Cl isotope under consideration; and S_1 is a summation over bcc lattice sites,

$$S_1 = \sum_k \left(\frac{a_0}{r_{jk}} \right)^6 \left[\frac{1}{2} (3 \cos^2 \theta_{jk} - 1) \right]^2. \quad (3)$$

Here r_{jk} is the distance between lattice sites j and k , and θ_{jk} is the angle between r_{jk} and H_0 , the external dc magnetic field. The factors 2 and 4 in Eqs. (1) and (2), respectively, refer to the number of F and Cl atoms in a molecule. S_1 has been calculated to be 5.809 for a powdered sample.¹² Evaluation of Eqs. (1) and (2) gives a total second moment $M_{2I} = 0.140$ G² as shown in Table II.

Now consider the case of a rigid lattice (i.e., all motions are slow compared to the inverse linewidth). The intramolecular contribution is easily calculated from the following expressions for a powder sample:

$$M_{2II}(\text{intra}) = 3I(I+1)\gamma_I^2 \hbar^2 \frac{1}{5} r_{j\bar{j}}^{-6}, \quad (4)$$

and

$$M_{2IS}(\text{intra}) = f_s \frac{4}{3} S(S+1)\gamma_S^2 \hbar^2 \frac{1}{5} \sum_{k=1}^4 r_{jk}^{-6}, \quad (5)$$

where the term $r_{j\bar{j}}$ in Eq. (4) is the F-F distance and in Eq. (5) the F-Cl distance, summed over the four Cl

nuclei in the molecule. These expressions are evaluated and given in Table II.

The calculation of the intermolecular contribution presents some problems. The orientations of the molecules are disordered, and thus we do not know the relative positions of nuclei. However, if we assume that the molecules are oriented *randomly* relative to each other (i.e., there are no preferred directions of orientation relative to each other), we can calculate the intermolecular contribution by averaging the second moment of each pair interaction over all possible orientations of the molecules. (Note that this is basically different from the previous case of rapid motion where we averaged the interaction rather than the second moment.) Thus, for a powder sample, we have

$$M_{2II}(\text{inter}) = 3I(I+1)\gamma_I^2 \hbar^2 \frac{1}{5} \sum_k \langle r_{j\bar{k}}^{-6} \rangle, \quad (6)$$

and

$$M_{2IS}(\text{inter}) = f_s \frac{4}{3} S(S+1)\gamma_S^2 \hbar^2 \frac{1}{5} \sum_k \langle r_{j\bar{k}}^{-6} \rangle, \quad (7)$$

where the summation in Eq. (6) is over I spins and in Eq. (7) is over S spins. The term $\langle r_{j\bar{k}}^{-6} \rangle$ is the average of $r_{j\bar{k}}^{-6}$ over all orientations of the two molecules to which spins j and k are attached. $\langle r_{j\bar{k}}^{-6} \rangle$ can be calculated by an integration over the surfaces of two spheres, S_j and S_k , generated by rotating the two molecules containing the j and k sites. Thus the radii R_j and R_k of the two spheres are the distances of the j and k sites from the centers of their respective molecules.

In the following paper,¹³ we carried out such an integration and from Eq. (42) of that paper, we obtain

$$\begin{aligned} \left\langle \left(\frac{a_0}{r_{j\bar{k}}} \right)^6 \right\rangle &= \oint_{S_j} dS_j \oint_{S_k} dS_k \left(\frac{a_0}{r_{j\bar{k}}} \right)^6 \\ &= \frac{a_0^6}{4R_j R_k} \int_{R_{jk}-R_j}^{R_{jk}+R_j} d\rho \int_{\rho-R_j}^{\rho+R_j} r^5 dr. \end{aligned} \quad (8)$$

Evaluating this integral, we have

$$\begin{aligned} \left\langle \left(\frac{a_0}{r_{j\bar{k}}} \right)^6 \right\rangle &= \left(\frac{a_0}{R_{jk}} \right)^6 \left[1 - R_{jk}^{-2}(R_j^2 + R_k^2) + R_{jk}^{-4} \left(\frac{14}{3} R_j^2 R_k^2 - R_j^4 - R_k^4 \right) \right. \\ &\quad \left. + R_{jk}^{-6} (R_j^6 + R_k^6 - R_j^4 R_k^2 - R_j^2 R_k^4) \right] \\ &\quad \times [1 - 2R_{jk}^{-2}(R_j^2 + R_k^2) + R_{jk}^{-4}(R_j^2 - R_k^2)^2]^{-3}. \end{aligned} \quad (9)$$

Thus, using Eq. (9) we evaluate Eqs. (6) and (7) and give the results in Table II.

One more contribution to the rigid-lattice second moment needs to be considered: that of the chemical shift

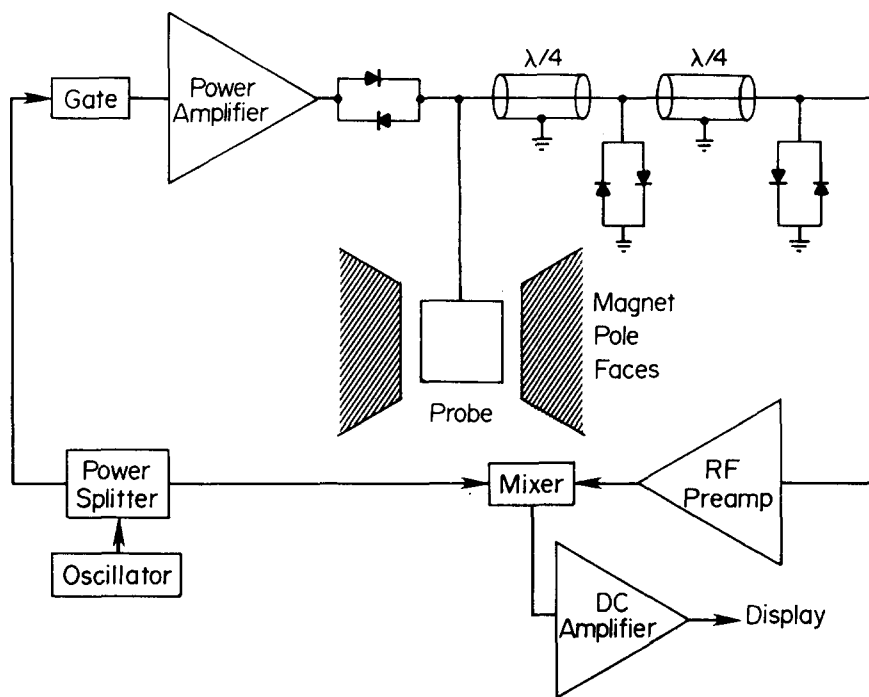


FIG. 1. Block diagram of pulse spectrometer.

anisotropy. Assuming axial symmetry in the chemical shift σ , we write

$$M_{2f}(\sigma) = \frac{4}{45}(\sigma_{\parallel} - \sigma_{\perp})^2 H_0^2, \quad (10)$$

where $\sigma_{\parallel} - \sigma_{\perp}$ has been measured⁷ in $\text{CFCl}_2\text{-CFCl}_2$ to be 2.4×10^{-4} . The evaluation of Eq. (10) is given in Table II.

Adding together all the contributions, we obtain a total second moment $M_{2f} = 0.75$ and 1.44 G^2 for the *trans* and *gauche* isomers, respectively, as shown in Table II. Since the crystal contains a mixture of *trans* and *gauche* isomers, the experimental second moment should lie somewhere in between.

The values calculated in Table II agree favorably with those calculated by Gutowsky and Takeda,⁶ Andrew and Tunstall,⁷ and Kishimoto.⁴ We differ only in the intermolecular contribution to the rigid-lattice value, which they only estimated. They then obtained different values for the *trans* and *gauche* isomers. Under our assumption of random orientation, we see clearly that the value should be independent of isomer, as shown in Table II.

III. EXPERIMENTAL PROCEDURES

The sample of $\text{CFCl}_2\text{-CFCl}_2$ was obtained originally from PCR, Inc. It was then purified and transferred to a glass tube where it was sealed under vacuum. (The details of this sample preparation are given in an earlier paper.¹⁴) Even though the sample was grown into a single crystal from the melt, it melted and recrystallized during the course of the NMR measurements. As a result, most of the data reported here was taken on a polycrystalline sample. However, because of the orientational disorder that exists in $\text{CFCl}_2\text{-CFCl}_2$, anisotropy effects in a single crystal are probably negligible. This is supported by the fact that we observed no anisotropy

(to within 10%) in T_{2f} at 116°K or in T_{1f} at 100°K in a freshly grown single crystal.

All of the NMR data was taken with a standard pulse spectrometer (see Fig. 1), using single-coil probes tuned to 50 Ω . Some of the T_1 data was taken using a transmission-line probe.¹⁵⁻¹⁷ This probe was constructed by winding 13 turns of copper ribbon (0.5 mm wide) on a 12-mm o.d. glass tube (see Fig. 2). This was covered with a layer of insulator (single layer of 0.5-mil Mylar obtained from a 400-V Mylar capacitor) and then with brass foil which was connected to ground. This arrangement gives the coil a distributed capacitance to ground and hence forms a transmission line,

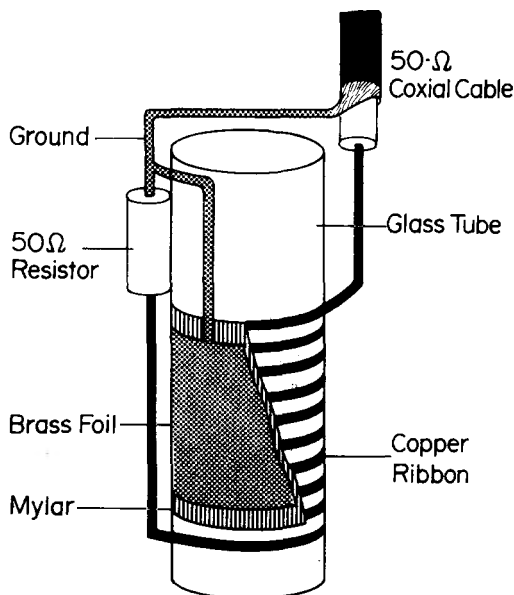


FIG. 2. Broadband NMR probe.

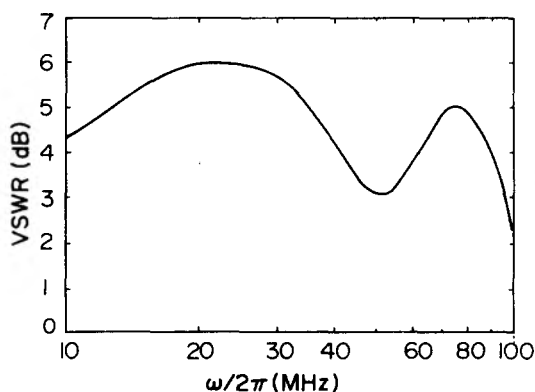


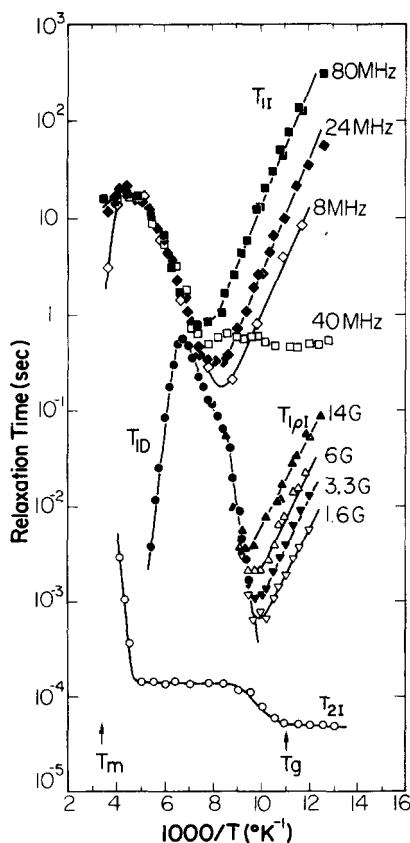
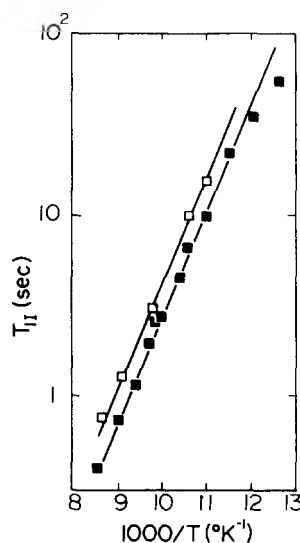
FIG. 3. The VSWR of the broadband NMR probe.

which, as we will see, has a characteristic impedance $Z_0 \approx 50 \Omega$. By terminating the coil with a $50\text{-}\Omega$ resistor connected to ground, the input impedance Z_{in} of the coil would be close to 50Ω over a wide range of frequency. We measured Z_{in} with a vector impedance meter as a function of frequency and expressed the result in terms of the voltage-standing-wave ratio (VSWR) in dB, using

$$\text{VSWR} = 20 \log_{10} \left[\frac{|Z_{in} + Z_0| + |Z_{in} - Z_0|}{|Z_{in} + Z_0| - |Z_{in} - Z_0|} \right], \quad (11)$$

where $Z_0 = 50 \Omega$.

Since the VSWR in Fig. 3 is small, the input impedance of the probe is fairly close to 50Ω over the entire frequency range shown. Using this probe in the pulse

FIG. 4. ^{19}F NMR relaxation data.FIG. 5. T_{1I} at 24 MHz. \square First day of measurements; \blacksquare subsequent measurements.

spectrometer, we could easily make NMR measurements over a wide range of frequencies. In particular, we measured the T_1 of ^{19}F in $\text{CFCl}_2\text{--CFCl}_2$ over the range 18–80 MHz. Using wide-band amplifiers, only the quarter-wavelength cables needed to be changed for different frequencies. We should note that none of the $T_{1\rho}$ or T_{1D} data were taken using this transmission-line probe.

IV. RESULTS

We measured the spin-lattice relaxation time T_{1I} , the rotating-frame relaxation time $T_{1\rho I}$, the dipolar relaxation time T_{1D} , and the spin-spin relaxation time T_{2I} of ^{19}F in $\text{CFCl}_2\text{--CFCl}_2$ over a wide temperature range (see Fig. 4). Kishimoto⁴ previously measured T_{1I} (at $\omega_{0I}/2\pi = 60$ MHz) and $T_{1\rho I}$ (at $H_{1I} = 5.42$ G) over approximately the same temperature range. For the most part, his measurements are consistent with our data but lack some of our detail. However, there are two major differences: (1) his $T_{1\rho I}$ data for $T \lesssim 100^\circ\text{K}$ has a much greater slope than ours, and (2) his T_{1I} data (60 MHz) for $T \lesssim 130^\circ\text{K}$ falls almost exactly on top of our T_{1I} data for 80 MHz and is thus shifted upward from our expected positions for 60 MHz data. Concerning this last point of disagreement, we observed ourselves a sample-history dependence of T_{1I} in this temperature region. On our first day of measurements, we obtained measurements of T_{1I} at 24 MHz, shown in Fig. 5 as open squares. Three days later, we took more measurements and found that T_{1I} was now significantly lower in value. These and all subsequent measurements (even months later) of T_{1I} at 24 MHz are shown in Fig. 5 as filled squares and fall on a straight line. Kishimoto's T_{1I} (60 MHz) data is consistent with our T_{1I} (24 MHz) data taken the first day.

In the following sections, we examine in detail some of the features of our NMR data and discuss its physical significance.

A. Second moments

We measured T_{2I} of the ^{19}F NMR free induction decay (FID) at 24 MHz as a function of temperature (see Fig.

4). At temperatures below about 90°K, we find $T_{2I} \cong 50$ μ sec. We observed the shape of the FID to be approximately Gaussian. (This is common for FID's in solids.^{18,19}) If we assume a Gaussian line shape, then we find

$$M_{2I} = 2/\gamma_I^2 T_{2I}^2. \quad (12)$$

Using $T_{2I} = 50$ μ sec, we obtain $M_{2I} = 1.26 \pm 0.08$ G². From Table II we see that this value is consistent with a rigid-lattice second moment arising from a mixture of the two isomers ($M_{2I} = 0.75$ and 1.44 G² for the *trans* and *gauche* isomers, respectively). Note that Gutowsky and Takeda⁶ measured $M_{2I} = 1.4$ G², and Andrew and Tunstall⁷ measured $M_{2I} = 1.3$ G² for this temperature region. (They reported 1.1 G² which had been corrected for chemical shift anisotropy.)

At about $T = 100^\circ\text{K}$, we see from Fig. 4 that T_{2I} increases (the line narrows) to a value $T_{2I} \cong 145$ μ sec. Using Eq. (12), we find that $M_{2I} = 0.13 \pm 0.01$ G². From Table II we see that this value agrees closely with the second moment for isotropic rotation ($M_{2I} = 0.140$ G²). Thus we conclude that the motion responsible for narrowing the line at $T \cong 100^\circ\text{K}$ is isotropic molecular reorientation. This is consistent with heat capacity measurements^{4,5} which indicate a "freezing out" of molecular reorientation at 90°K. Note that Gutowsky and Takeda⁶ measured $M_{2I} = 0.18$ G² for this temperature region.

At $T = 200^\circ\text{K}$, we see from Fig. 4 another increase in T_{2I} , this time due to translational self-diffusion which we will discuss in the next section.

B. Translational self-diffusion

In plastic crystals, translational self-diffusion usually becomes a dominant spin-lattice relaxation mechanism near the melting point. Such is also the case in CFCl_2 - CFCl_2 (see Fig. 4). This occurs in the temperature region of rapid molecular reorientation, where, as discussed in Sec. II, the intramolecular dipolar interactions are averaged to zero and the intermolecular interactions are averaged to values which one would obtain by placing all spins at the centers of their respective molecules. Thus, in this case, theories for relaxation in monoatomic crystals may be applied.

The dominant self-diffusion mechanism in plastic crystals is thought to be motion of vacancy defects.²⁰⁻²² Accordingly, we will use relaxation theories for vacancy diffusion in a monoatomic bcc lattice of a polycrystalline sample. It is evident from Fig. 4 that all the data is on the low-temperature side of the T_{1I} minima. Thus, we need expressions for relaxation times only in the limit $\omega_0 \tau_d \gg 1$, where τ_d is the average time between diffusion jumps of a molecule.

For high-field relaxation, we obtain from the random-walk theory of Wolf²³

$$T_{1I}^{-1} = 2 \times \frac{3}{8} \gamma_I^4 \hbar^2 I(I+1) \omega_{0I}^2 \tau_d^{-1} a_0^{-6} (25.6), \quad (13)$$

$$T_{2I}^{-1} = 2 \times \frac{3}{8} \gamma_I^4 \hbar^2 I(I+1) \tau_d a_0^{-6} (39.0). \quad (14)$$

Furthermore,

$$T_{1\rho I}^{-1} = T_{2I}^{-1}, \quad (15)$$

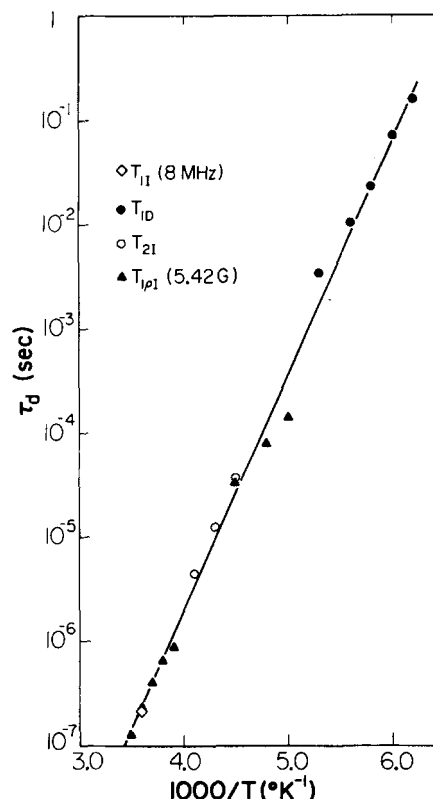


FIG. 6. Jump time τ_d for translational self-diffusion.

in the limit $\omega_{1I} \tau_d \ll 1$, and

$$T_{1\rho I}^{-1} = 2 \times \frac{3}{8} \gamma_I^4 \hbar^2 I(I+1) \omega_{1I}^2 \tau_d^{-1} a_0^{-6} (18.9), \quad (16)$$

in the limit $\omega_{1I} \tau_d \gg 1$. In the above expressions, $\omega_{1I} = \gamma_I H_{1I}$, where H_{1I} is the magnitude of the rf field applied at frequency ω_{0I} . A factor 2 was included in Eqs. (13)–(16) to account for the two fluorine nuclei in each molecule of CFCl_2 - CFCl_2 . The F-Cl dipolar interactions are negligible here and are thus neglected. Note that our a_0 as defined in this paper is twice the a_0 in Ref. 23.

For low field relaxation, we obtain from the encounter model²⁴

$$T_{1D}^{-1} = \tau_d^{-1} (0.822) \quad (17)$$

in the limit $\tau_d \gg T_{2I}$.

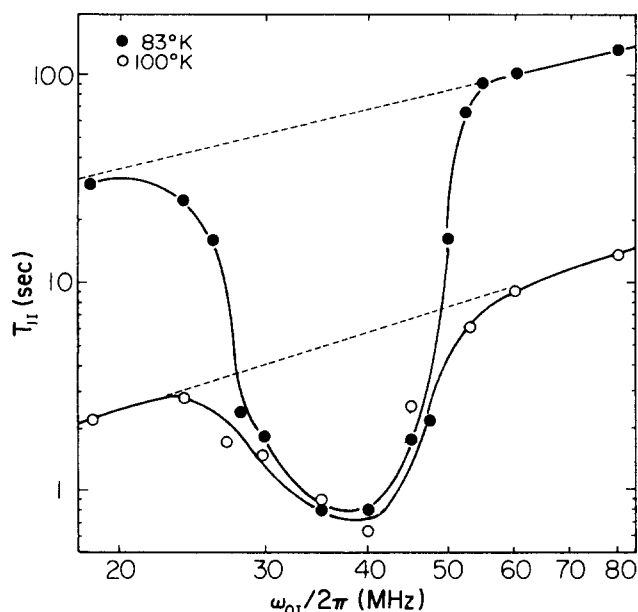
Using Eqs. (13)–(17) we can calculate τ_d from the experimental values of T_{1I} , T_{2I} , and T_{1D} . (We also included the $T_{1\rho I}$ data of Kishimoto.⁴) As seen in Fig. 6, over six decades the result exhibits Arrhenius behavior,

$$\tau_d = \tau_0 \exp(E_A/kT), \quad (18)$$

where $\tau_0 = 2.0 \times 10^{-15}$ sec and the activation energy $E_A = 43.0 \pm 0.3$ kJ/mole. From linewidth measurements, Kishimoto⁴ obtained $E_A = 44$ kJ/mole for self-diffusion.

C. Zeeman-quadrupole cross relaxation

At low temperatures, we observed in T_{1I} at 40 MHz anomalous behavior (see Fig. 4) which we attribute to cross relaxation between the Zeeman levels of the ¹⁹F spins and the quadrupole levels of the ³⁵Cl and ³⁷Cl

FIG. 7. Effect of Zeeman-quadrupole cross relaxation on T_{1I} .

spins. This cross relaxation causes a large reduction in the apparent T_{1I} . Similar effects have been observed in a number of experiments.²⁵⁻³¹ To investigate this effect further, we measured T_{1I} as a function of ω_{0I} at two different temperatures (see Fig. 7) and observed a broad minimum in T_{1I} centered at about 40 MHz. Assuming that the quadrupolar T_{1S} is much less than the cross relaxation time τ_{IS} , we see that the apparent reduction in T_{1I} is limited by τ_{IS} . (Actually, the relaxation time is limited by the sum, $\tau_{IS} + T_{1S}$, where T_{1S} is the spin-lattice relaxation time of the chlorines. Normally, for quadrupolar relaxation, T_{1S} is very short and can be neglected compared to τ_{IS} .) In particular,

$$T_{1I}^{-1} = \tau_{IS}^{-1} + T_{1I}^{-1}(\text{normal}), \quad (19)$$

where $T_{1I}(\text{normal})$ is the "normal" spin-lattice relaxation time shown as the dashed line in Fig. 7. By subtracting $T_{1I}^{-1}(\text{normal})$ from T_{1I}^{-1} , we obtain τ_{IS}^{-1} , which we plot in Fig. 8. Note that τ_{IS} is temperature independent as we would expect.

Generally, cross relaxation occurs at fields H_0 where the Zeeman splitting ω_{0I} of the I spins is equal to the quadrupolar splitting ω_{QS} of the S spins. Of course, the presence of H_0 also splits the quadrupole resonance and, in the case of $\text{CFCl}_2\text{-CFCl}_2$ where the molecules are orientationally disordered, broadens the quadrupole resonance considerably, making it possible to satisfy the cross relaxation condition $\omega_{0I} = \omega_{QS}$ over a wide range of ω_{0I} . Hence we see a very broad minimum in τ_{IS} (Fig. 8).

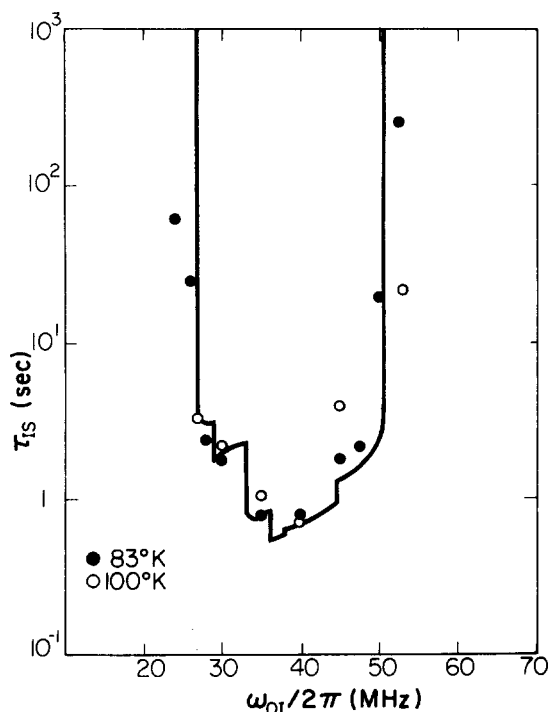
We derived a theoretical expression for the cross relaxation time τ_{IS} (see the following paper¹³). All parameters in the theory are well-known physical constants except for ω_{QS} , the quadrupole splitting of ^{35}Cl and ^{37}Cl . Using a pulse NQR spin-echo technique,³² we attempted to find directly the pure quadrupole resonance of ^{35}Cl at 77°K and thus determine ω_{QS} . We were unable to find this resonance, possibly because of the line broadening

due to random orientations of the $\text{CFCl}_2\text{-CFCl}_2$ molecules in the glassy crystalline phase. From NQR measurements in other chlorinated ethanes³³⁻³⁵ we find that generally $\omega_{QS}/2\pi \cong 40$ MHz for ^{35}Cl in these compounds. Using this value (and hence $\omega_{QS}/2\pi = 31.5$ MHz for ^{37}Cl), we calculated τ_{IS} (see the following paper¹³) and plotted the result as a solid line in Fig. 8. Considering that there are no adjustable parameters in the theoretical calculation, the agreement with experimental data is excellent.

The cross relaxation effect disappears at $T \geq 125^\circ\text{K}$. In this temperature region, the rate of molecular reorientation is greater than 40 MHz and the Cl quadrupole splitting is thus motionally narrowed and "smeared" out (see pp. 67-68 in Ref. 36).

D. Molecular reorientation

At low temperatures (below 200°K for T_{1I} and below 150°K for $T_{1\rho I}$ and T_{1D}) we find some very unusual relaxation phenomena (see Fig. 4). Perhaps one of the most striking features present is the reduced field dependence on the cold side of the minima. If we plot, for example, $\ln T_{1\rho I}$ vs $\ln H_{1I}$ at $T = 83^\circ\text{K}$ (see Fig. 9), we find it falls on a straight line with a slope $\alpha \cong 1$. This means that approximately $T_{1\rho I} \propto H_{1I}$. Similarly, from a plot of $\ln T_{1I}$ vs $\ln \omega_{0I}$ at $T = 100^\circ\text{K}$ (the lower dashed line in Fig. 7), we obtain $T_{1I} \propto H_0^\alpha$ with $\alpha \cong 1.2$. Furthermore, the field dependence between the T_{1I} and $T_{1\rho I}$ data also follows an approximate relation $T_{1I}/T_{1\rho I} \cong (H_0/H_{1I})^\alpha$, only with $\alpha \cong 1.1$. The field dependence of T_{1I} and $T_{1\rho I}$ is thus self-consistent and indicates that both T_{1I} and $T_{1\rho I}$ are probably due to the same relaxation mechanism in this temperature region. This conclusion is further supported by the fact that the T_{1I} and

FIG. 8. The cross relaxation time τ_{IS} as a function of ω_{0I} .

$T_{1\rho I}$ data have similar slopes: 11.7 and 9.5 kJ/mole, respectively.

The values of T_{1I} and $T_{1\rho I}$ at their minima also follow an unusual field dependence. Plotting in $T_{1\rho I, \min}$ vs $\ln H_{1I}$ (see Fig. 10), we see that $T_{1\rho I, \min} \propto H_{1I}^\beta$ with $\beta = 0.83 \pm 0.05$. Also, from the ratio of the T_{1I} values at their minima at 80 and 24 MHz, we find $T_{1I, \min} \propto H_0^\beta$ with $\beta = 0.76 \pm 0.05$. Again, the similar field dependence of $T_{1\rho I, \min}$ and $T_{1I, \min}$ is further evidence of a single relaxation mechanism for both $T_{1\rho I}$ and T_{1I} .

Another unusual aspect of the relaxation data is the large asymmetry in slopes on the two sides of the $T_{1\rho}$ minima. The slope on the hot side of the minima (33 kJ/mole) is more than three times the slope on the cold side. It appears that this asymmetry cannot simply be explained just in terms of an additional relaxation mechanism.

Now we note that the low-field $T_{1\rho I}$ minima occur near the onset of motional narrowing at $T \approx 100^\circ\text{K}$. This suggests³⁷ that the same motion which is narrowing the line at 100°K is also responsible for the $T_{1\rho I}$ relaxation. In Sec. IV A we showed that this motion is indeed molecular reorientation. Thus we conclude that the relaxation mechanism responsible for T_{1I} and $T_{1\rho I}$ in the low temperature region is likewise molecular reorientation.

This conclusion is in some ways not surprising since one often finds in plastic crystals that molecular reorientation provides a strong relaxation mechanism at low temperatures. However, one usually also finds that the relaxation data is consistent with a Bloembergen, Purcell, and Pound-type theory³⁸ (BPP), i.e.,³⁹

$$\frac{1}{T_{1I}} = \frac{2}{3} \gamma_I^2 \Delta M_{2II} \left[\frac{\tau_r}{1 + \omega_{0I}^2 \tau_r^2} + \frac{4\tau_r}{1 + 4\omega_{0I}^2 \tau_r^2} \right], \quad (20)$$

and

$$\frac{1}{T_{1\rho I}} = \frac{2}{3} \gamma_I^2 \Delta M_{2II} \left[\frac{3}{2} \frac{\tau_r}{1 + 4\omega_{0I}^2 \tau_r^2} + \frac{5}{2} \frac{\tau_r}{1 + \omega_{0I}^2 \tau_r^2} + \frac{\tau_r}{1 + 4\omega_{0I}^2 \tau_r^2} \right], \quad (21)$$

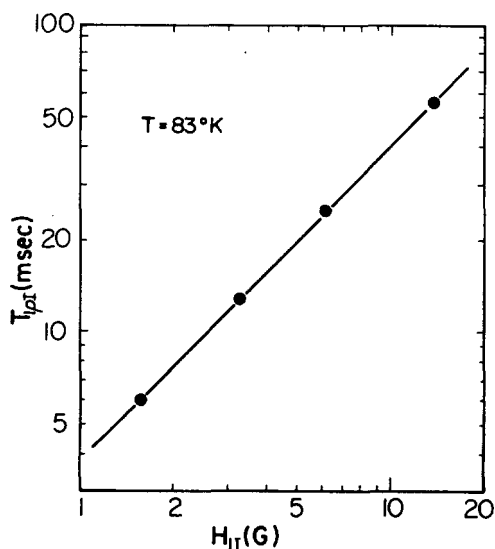


FIG. 9. $T_{1\rho I}$ as a function of H_{1I} at 83°K . The line is a best fit to the data.

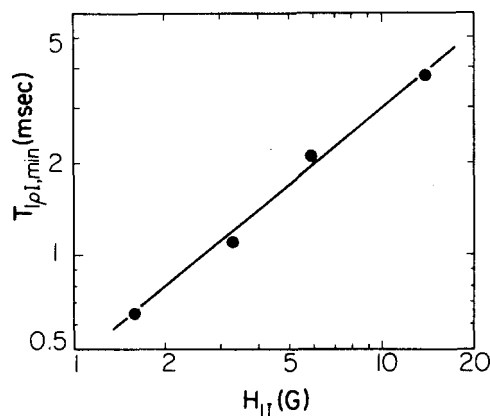


FIG. 10. $T_{1\rho I, \min}$ as a function of H_{1I} . The line is a best fit to the data.

where τ_r is the correlation time of the reorientation and ΔM_{2II} is the part of M_{2II} which is modulated by the reorientation. These expressions have been successfully used in NMR studies of a number of plastic crystals.⁴⁰⁻⁴⁵

Our data follows some of the general aspects of the BPP-type theories given by Eqs. (20) and (21). T_{1I} and $T_{1\rho I}$ are field independent on the hot side of the minima ($\omega_{0I}\tau_r \ll 1$ and $\omega_{1I}\tau_r \ll 1$) and are field dependent on the cold side of the minima ($\omega_{0I}\tau_r \gg 1$ and $\omega_{1I}\tau_r \gg 1$) with T_{1I} and $T_{1\rho I}$ increasing with increasing field. However, in some ways, our data deviates substantially from this theory. Equations (20) and (21) predict that $T_{1I} \propto H_0^2$ and $T_{1\rho I} \propto H_{1I}^2$ on the cold side of the minima and that $T_{1I, \min} \propto H_0$ and $T_{1\rho I, \min} \propto H_{1I}$. Furthermore, they predict that the slopes of each relaxation time are equal in magnitude on both sides of the minimum. As we have already pointed out in this section, our data departs sharply from these predictions of Eqs. (20) and (21).

We are not presently able to explain these phenomena theoretically. However we briefly discuss here a couple of possibilities. First of all, consider the possibility that these features arise from the nature of the motion involved in the molecular reorientation process. As an example, Walstedt *et al.*⁴⁶ measured T_1 of ^{23}Na in Na β -alumina at 17.2 and 25.5 MHz. They observed an asymmetry in the slopes on the two sides of the T_1 minima and also observed on the cold side of the minima a field dependence which is substantially less than the BPP-type field-squared dependence. They explained their data in terms of a distribution $G(E_A)$ of heights of the barriers to the motion. Assuming that, at each value of E_A , their relaxation follows a BPP-type behavior, they obtained

$$\frac{1}{T_1} \propto \int dE_A \frac{G(E_A)\tau}{1 + \omega_0^2 \tau^2}. \quad (22)$$

Using an appropriate distribution function $G(E_A)$, they were able to make a good fit of Eq. (22) to their data. We would find it much more difficult to fit such a theory to our data, since our unusual field dependence covers a range of over four orders of magnitude in field ($H_{1I} = 1.6 \text{ G}$ to $H_0 = 20 \text{ kG}$). (It should be noted that a reduced field dependence of T_1 has also been observed by others^{47,48} in some polymers.)

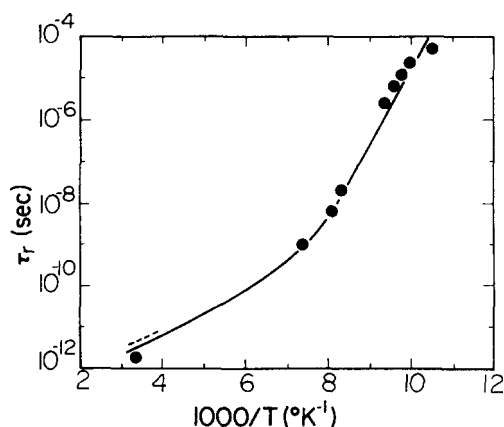


FIG. 11. Correlation time τ_r of the molecular reorientation. The dashed line is from Ref. 5.

Another approach to the explanation of our data may involve the nature of the *interaction* itself rather than the motion. For example, each fluorine nucleus in $\text{CFCl}_2\text{--CFCl}_2$ is in close proximity to *two* chlorine nuclei. As we commented in the previous section, the Cl quadrupolar relaxation time T_{1S} is normally very short. The modulation of S due to T_{1S} processes can cause I – S spin relaxation via the I – S dipolar interaction. Such an indirect relaxation process has been called “dipolar relaxation of the second kind”⁴⁹ and has been observed in a number of cases.^{49–54} A field-squared dependence typically has been observed^{49–52} for this kind of relaxation. However, these observations have been made in systems undergoing motional narrowing. In our case of “slow” motion where $T_{1S} \approx \tau_r$ (see Ref. 55), it may be possible to obtain a different result which could produce some unusual features in $T_{1\rho I}$ and T_{1I} , such as the ones that we have observed.

Even though we do not have a theory to explain our data, we can still learn something about the general behavior of the correlation time τ_r of the molecular reorientation. First of all, we know that $\tau_r \approx T_{2I}$ at the onset of motional narrowing. Thus we obtain $\tau_r = 50 \mu\text{sec}$ at $T = 95^\circ\text{K}$. Second, we know that $\omega_{1I}\tau_r \approx 1$ at the $T_{1\rho I}$ minima and $\omega_{0I}\tau_r \approx 1$ at the T_{1I} minima. Hence we obtain approximate values of τ_r at those points. In addition, we measured T_{2S} of the ^{35}Cl NMR FID at 8 MHz near the melting point T_m and obtained $T_{2S} \approx 20 \mu\text{sec}$. Such a short T_{2S} is caused by lifetime broadening due to a strong quadrupolar relaxation in rapidly tumbling molecules. For this case of extreme narrowing, we have⁵⁶ for $S = \frac{3}{2}$,

$$T_{2S}^{-1} = T_{1S}^{-1} = 0.4\omega_Q^2\tau_r, \quad (23)$$

from which we obtain $\tau_r = 2.0 \times 10^{-12}$ sec. We plot these values of τ_r obtained from T_{2I} , the $T_{1\rho I}$, and T_{1I} minima, and T_{2S} in Fig. 11. Satija and Wang¹⁴ also obtained values of τ_r from depolarized Rayleigh scattering data over the range $T = 265$ to 297°K . Their results are shown as a dashed line in Fig. 11 and are seen to be in fair agreement with our T_{2S} result.

We now have in Fig. 11 the general behavior of τ_r over a wide range of temperature. As we can see, the

activation energy E_A is not constant but seems to increase with decreasing temperature. Near the melting point, light scattering data¹⁴ gives $E_A \approx 7.3 \pm 0.5$ kJ/mole. At low temperatures, we can see from Fig. 11 that $E_A = 35$ kJ/mole. Note that we could not obtain E_A directly from the slopes of the T_{1I} and $T_{1\rho I}$ data without knowing their τ dependences. For example,⁵⁷ any relationship of the type $T_{1I} \propto \tau^\nu$ would give us a straight line on a plot of $\ln T_{1I}$ vs T^{-1} (as we observed) but with a slope νE_A . Without a theory to explain the data, we do not know the value of ν and thus cannot determine E_A from the slope of the T_{1I} data.

Note that there seems to be a sudden change in E_A near $T = 125^\circ\text{K}$. This is very close to the temperature where the conversion between the *trans* and *gauche* conformers are frozen out ($T = 130^\circ\text{K}$). Thus these two phenomena may be related.

ACKNOWLEDGMENTS

We thank Dr. S. K. Satija for his assistance in preparing the samples used in this work. We also thank Professor G. A. Williams for generously allowing us the use of some of his facilities. We appreciate the assistance of Professor J. S. Ball in the computer analysis of some of the data. Lastly, we appreciate helpful discussions with Dr. J. B. Boyce, Professor B. G. Dick, Professor H. S. Gutowsky, Professor E. L. Hahn, Dr. C. E. Hayes, Dr. A. R. King, Dr. J. Piott, Dr. M. Polak, Dr. M. Rubinstein, Professor C. P. Slichter, Professor J. H. Strange, Professor R. W. Vaughan, and Dr. D. Wolf.

This work was supported by the NSF under Grant DMR 76-18966. One of the authors (C.H.W.) was supported by the Petroleum Research Fund, sponsored by the American Chemical Society.

¹J. Timmermans, *J. Phys. Chem. Solids* **18**, 1 (1961).

²H. Suga and S. Seki, *J. Non-Cryst. Solids* **16**, 171 (1974).

³K. Adachi, H. Suga, and S. Seki, *Bull. Chem. Soc. Jpn.* **41**, 1073 (1968).

⁴K. Kishimoto, Ph.D. thesis, Osaka University, 1976 (unpublished).

⁵K. Kishimoto, H. Suga, and S. Seki, *Bull. Chem. Soc. Jpn.* **51**, 1691 (1978).

⁶H. S. Gutowsky and M. Takeda, *J. Phys. Chem.* **61**, 95 (1957).

⁷E. R. Andrew and D. P. Tunstall, *Proc. Phys. Soc. London* **81**, 986 (1963).

⁸M. Iwasaki, S. Nagase, and R. Kojima, *Bull. Chem. Soc. Jpn.* **30**, 230 (1957).

⁹G. W. Smith, *J. Chem. Phys.* **36**, 3081 (1962).

¹⁰L. V. Dmitrieva and V. V. Moskalev, *Fiz. Tverd. Tela* **5**, 2230 (1963) [*Sov. Phys. Solid State* **5**, 1623 (1964)].

¹¹D. J. Kroon, *Philips Res. Rep.* **15**, 501 (1960).

¹²H. T. Stokes and D. C. Ailion, *Phys. Rev. B* **15**, 1271 (1977).

¹³H. T. Stokes and D. C. Ailion, *J. Chem. Phys.* **70**, 3572 (1979), following paper.

¹⁴S. K. Satija and C. H. Wang, *J. Chem. Phys.* **69**, 1101 (1978).

¹⁵A. R. King, Ph.D. thesis, University of California at Berkeley, 1972 (unpublished).

¹⁶I. J. Lowe and M. Engelsberg, *Rev. Sci. Instrum.* **45**, 631 (1974).

- ¹⁷I. J. Lowe and D. W. Whitson, *Rev. Sci. Instrum.* **48**, 268 (1977).
- ¹⁸B. T. Gravely and J. D. Memory, *Phys. Rev. B* **3**, 3426 (1971).
- ¹⁹M. Engelsberg and I. J. Lowe, *Phys. Rev. B* **10**, 822 (1974).
- ²⁰R. Folland, R. L. Jackson, J. H. Strange, and A. V. Chadwick, *J. Phys. Chem. Solids* **34**, 1713 (1973).
- ²¹A. V. Chadwick, J. M. Chezeau, R. Folland, J. W. Forrest, and J. H. Strange, *J. Chem. Soc. (London) Faraday Trans. I* **71**, 1610 (1975).
- ²²N. Boden, J. Cohen, and R. T. Squires, *Mol. Phys.* **31**, 1813 (1976).
- ²³D. Wolf, *J. Magn. Reson.* **17**, 1 (1975).
- ²⁴D. Wolf, *Phys. Rev. B* **10**, 2724 (1974).
- ²⁵M. Goldman, *C. R. Acad. Sci. (Paris)* **246**, 1038 (1958).
- ²⁶D. E. Woessner and H. S. Gutowsky, *J. Chem. Phys.* **29**, 804 (1958).
- ²⁷G. P. Jones and J. T. Daycock, *J. Phys. C* **4**, 765 (1971).
- ²⁸Y. Hsieh, J. C. Koo, and E. L. Hahn, *Chem. Phys. Lett.* **13**, 563 (1972).
- ²⁹D. E. Demco, S. Kaplan, S. Pausak, and J. S. Waugh, *Chem. Phys. Lett.* **30**, 77 (1975).
- ³⁰M. Shporer and A. M. Achlama, *J. Chem. Phys.* **65**, 3657 (1976).
- ³¹G. Voigt and R. Kimmich, *J. Magn. Reson.* **24**, 149 (1976); R. Kimmich, *Z. Naturforsch. A* **32**, 544 (1977).
- ³²M. Rubinstein and P. C. Taylor, *Phys. Rev. B* **9**, 4258 (1974).
- ³³R. Livingston, *J. Chem. Phys.* **20**, 1170 (1952).
- ³⁴R. Livingston, *J. Phys. Chem.* **57**, 496 (1953).
- ³⁵S. Kondo, *Bull. Chem. Soc. Jpn.* **39**, 249 (1966).
- ³⁶T. P. Das and E. L. Hahn, in *Solid State Physics*, edited by F. Seitz and D. Turnbull (Academic, New York, 1958), Suppl. 1.
- ³⁷D. C. Ailion, in *Advances in Magnetic Resonance*, edited by J. S. Waugh (Academic, New York, 1971) Vol. 5, pp. 177-227.
- ³⁸N. Bloembergen, E. M. Purcell, and R. V. Pound, *Phys. Rev.* **73**, 679 (1948).
- ³⁹G. Soda and H. Chihara, *J. Phys. Soc. Jpn.* **36**, 954 (1974).
- ⁴⁰J. M. Chezeau, J. Dufourcq, and J. H. Strange, *Mol. Phys.* **20**, 305 (1971).
- ⁴¹R. L. Jackson and J. H. Strange, *Mol. Phys.* **22**, 313 (1971).
- ⁴²S. Albert and J. A. Ripmeester, *J. Chem. Phys.* **57**, 3953 (1972).
- ⁴³S. Albert, H. S. Gutowsky, and J. A. Ripmeester, *J. Chem. Phys.* **64**, 3277 (1976).
- ⁴⁴H. A. Resing, *Mol. Cryst. Liq. Cryst.* **9**, 101 (1969).
- ⁴⁵J. G. Powles, A. Begum, and M. O. Norris, *Mol. Phys.* **17**, 489 (1969).
- ⁴⁶R. E. Walstedt, R. Dupree, J. P. Remeika, and A. Rodriguez, *Phys. Rev. B* **15**, 3442 (1977).
- ⁴⁷A. W. Nolle and J. J. Billings, *J. Chem. Phys.* **30**, 84 (1959).
- ⁴⁸R. Lenk, *Adv. Mol. Relax. Processes* **3**, 3 (1972).
- ⁴⁹M. O. Norris, J. H. Strange, J. G. Powles, M. Rhodes, K. Marsden, and K. Krynicki, *J. Phys. C* **1**, 422 (1968); *J. Phys. C* **1**, 445 (1968).
- ⁵⁰J. H. Strange and M. Terenzi, *J. Phys. Chem. Solids* **33**, 923 (1972).
- ⁵¹N. Bloembergen and P. P. Sorokin, *Phys. Rev.* **110**, 865 (1958).
- ⁵²R. L. Armstrong, J. A. J. Lourens, and K. R. Jeffrey, *J. Magn. Reson.* **23**, 115 (1976).
- ⁵³D. J. Genin, D. E. O'Reilly, E. M. Peterson, and T. Tsang, *J. Chem. Phys.* **46**, 4525 (1968).
- ⁵⁴S. Albert and J. A. Ripmeester, *J. Chem. Phys.* **59**, 1069 (1973).
- ⁵⁵S. Alexander and A. Tzalmona, *Phys. Rev. A* **138**, 845 (1965).
- ⁵⁶A. Abragam, *The Principles of Nuclear Magnetism* (Clarendon, Oxford, England, 1961), p. 314.
- ⁵⁷R. Lenk, *Adv. Mol. Relax. Processes* **6**, 287 (1975).